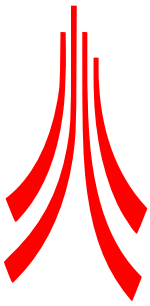

University of Lancaster

PHYS352 - Short Project III

Second Sound in Superfluid Helium

Author:
Matthew Sarsby

Director of Studies:
Dr. Edward McCan

March 20, 2011

Abstract

Using resonances generated by a coil heater and detected with a Allen-Bradley resistor and a phase detector, the presence of second sound was observed on an oscilloscope. Inside a tube of length 72 ± 1mm, the resonances were used to measure the velocity of second sound in superfluid ^{4}He-II at 1.46K, in a undergraduate lab, to be $v = (19.8372 \pm 0.2761)\text{ms}^{-1}$. Also observed are the node–antinode structure of the resonance of second sound, and by varying temperature the drop in velocity to zero when temperature approaches the transition temperature.

Contents

1 Introduction

Second sound is the propagation of heat in waves through superfluid. Heat waves can be created with cyclic I^2R heating on a resistive coil, and measured with an Allen Bradley carbon resistor.

The velocity will be measured in a cryogenic environment using resonance at a fixed temperature with different harmonics for added accuracy, then the cryogenic environment is allowed to heated up and the frequency of the $n = 1$ fundamental harmonic frequency is tracked.

This report the experiment is split into: cooling the apparatus and helium to a superfluid and measuring the temperature for calibration when warming back up; resonance of the the superfluid with I^2R heating for different harmonic frequency inside of a resonance chamber in the cryogenic environment, with which the velocity of the second sound is calculated; and finally the fundamental frequency changing over temperature.

1.1 History

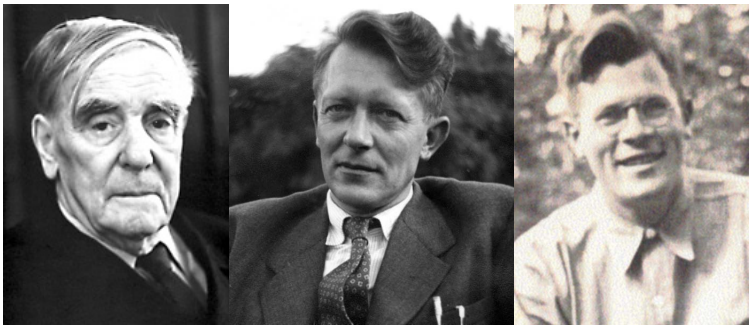

Pjotr Leonidovich Kapitsa | John "Jack" Frank Allen | Don Misener

Figure 1.1: Physisics discovering Superfluidity in Helium in 1937.

Don Misener (a graduate of University of Toronto) and John F. Allen from Winnipeg Canada[1] (a graduate of University of Manitoba) discovered the superfluid phase of matter in 1937 using liquid helium in the Royal Society Mond Laboratory in Cambridge, with there work published in nature 141, 75 [2]. Byt also in 1937 Pyotr Leonidovich Kapitsa (a.k.a. Peter Kapitza) 1894 - 1984 a Soviet Russian Physicist released a paper Nature 141 74 in the same January 8th 1938 issue of Nature journal as J F Allen and D Misener. Both of the studies demonstrated no viscosity below a 'transition temperature of 2.18K.

It was 40 years before the Nobel Orgnization[3] awarded half of that current years Nobel Prize for Physics to P. Kapitsa for his " basic inventions and discoveries in the area of low-temperature physics". The work

from the Mond Laboratory did not get the same recognition other than a single sentence in the Nobel Citation. An interesting read on the controversy is available on `www.physics.utoronto.ca/~griffin/PW%20article%20griffin.pdf`

1.2 Relavance

Superfluids are a relatively new field, less than 80 years old. Interesting systems that have a superfluids behaviour are, for example, rarefied cold atomic gasses with both fermions and bosons, electrons in superconductors, and it is thought that neutron stars are thought be be a fermionic superfluid.

2 Theory

2.1 Cryogenics

cryogenics roughly translates to "the production of icy cold" or the "branch of physics which deals with the production of very low temperatures and their effect on matter – Oxford English Dictionary, 2nd edition, Oxford University Press (1989). It is informally considered anything below around 170K.

2.2 Cryogenic Cooling

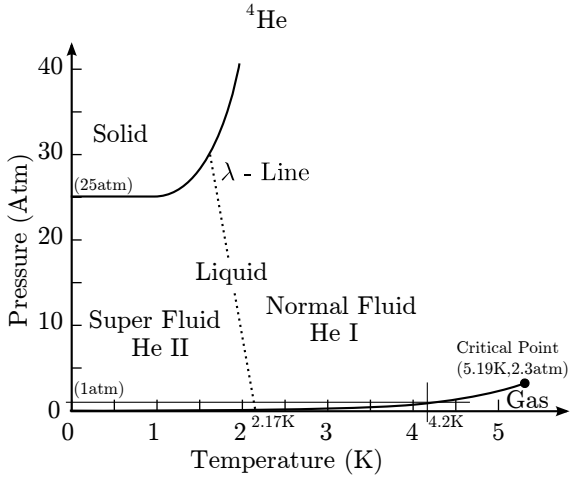

Figure 2.1: P-V diagram for helium-4.

Starting with a liquid helium sample in a cryostat it is possible to cool to lower temperatures by exploiting the phase transition lines as shows in a diagram in Figure 2.1. The sample ^{4}He is liquid in contact with vapour ^{4}He. As the sample is equilibrium it must lie on the phase transition line of liquid to vapour. By attaching a vacuum pump and slowly pumping on the vapour the pressure is reduced, as the pressure goes down the sample is still in equilibrium on the phase line, so the boiling point, and temperature, of the sample goes down, on Figure 2.1 this is a down and to the left direction. The vapour pressures and corresponding temperatures of the ^{4}He have been measured so that in the following experiment low temperature thermometry not a complication and the pressure measurements can be converted into temperatures.

The theoretical limit of cooling it at $T = 0$K, although imposable to reach. There is still energy in the system, called zero-point energy. ^{4}He is special because even at 0K the Van Der Walls forces (Figure) between the atoms are too strong to cause ^{4}He to become solid.

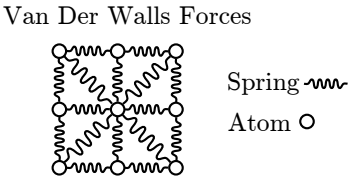

Figure 2.2: Van Der Walls forces acting as springs between atoms

2.3 Superfluids

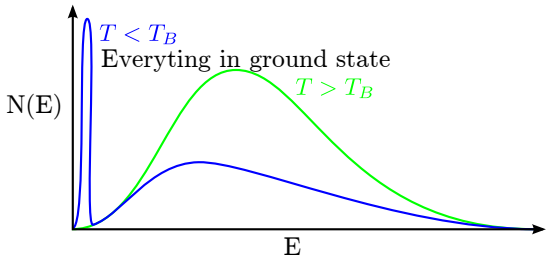

Figure 2.3: Qualitative graph showing how the distribution N of atoms depending on energy E, $N(E)$ changes between two example temperatures above a transition point, here labeled T_B. The large peak at low E is intended to show ground state occupation.

Helium 4 is a "composite boson" with net spin of zero, made of just two protons, two neutrons, and two electrons. As a boson it mostly follows Bose-Einstein statistics and at low temperatures Bose-Einstein condensation describes the formation of superfluid as atoms 'condense to the ground energy state and become indistinguishable. The mass condensation of atoms to the ground state leads to a macroscopic occupation of the ground state.

The transition to ground state begins at a lambda point. Below the lambda point helium (^{4}He) becomes superfluid. Called ^{4}HeII above the lambda point and below called ^{4}HeI, for first (I) and second (II) state of liquid ^{4}He.

An property of ^{4}He-II is the apparent loss of all viscosity, figure 2.4.

At the transition point the heat capacity of the system dramatically increases, Figure 2.5. The peak of the heat capacity is rounded by other fields adding potentials across the fluid.

In the laboratory, it is the height of the superfluid and the gravitational potential energy across the container that add a small variation of the ground state energy[1]. Because of the This 'rounding' of the ground state is enough to make the transition surmountable[4].

[1]In space, where the potential from gravity changes less across the container, the Cv peak is much higher, as tested on the ISS

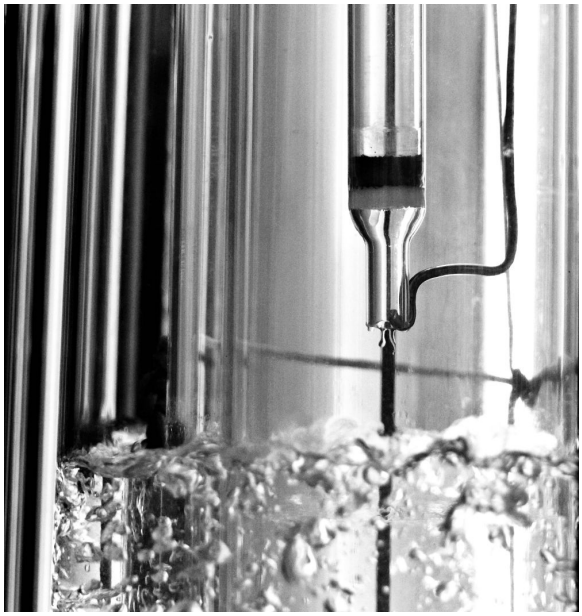

Figure 2.4: Photograph of superfluid in a demonstration cryostat (clear glass) having just passed through a superleak, a fluid with only zero viscosity can do.

2.4 Cryostat Design

Cryostats are designed to reduce the heat flow $\dot{Q}$ from the laboratory environment, at ≈ 300K, to the cryogenic liquid, $\approx 2 \rightarrow 4$K.

Dewars themselves are good insulators from conduction as the vacuum between the glass layers actually gets better under lower temperature, the renaming gas in the vacuum will 'stick' (energetically beneficial) to the colder surface and no longer shuttle heat between the two vacuum surfaces.

To reduce the black body radiation heating up the Helium the outer surface of the dewars are coated in a shiny metallic foil.

$$\dot{Q}_{\text{blackbody}} = \sigma \epsilon A T^4 \tag{2.1}$$

σ is the Stephan Boltzmann constant at 5.68×10^{-8}, and ϵ is the emissivity of the surface, a value that changes between 0 for a none emitting surface, and 1 for a perfect black body. By reducing the emissivity, ϵ, of the glass by coating it in silver, the total amount of heat $\dot{Q}$ it absorbs from radiation.

Equation 2.1 is only for the black body radiation in one direction, Black body radiation is a a two way process, absorption of heat $\dot{Q}_{\text{in}}$ from black body radiation and the emission of heat $\dot{Q}_{\text{out}}$ with the same process. So the total heat absorbed is Equation 2.2.

$$\dot{Q}_{\text{total}} = \sigma \epsilon A \left(T_{\text{hot}}^4 - T_{\text{cold}}^4 \right) \tag{2.2}$$

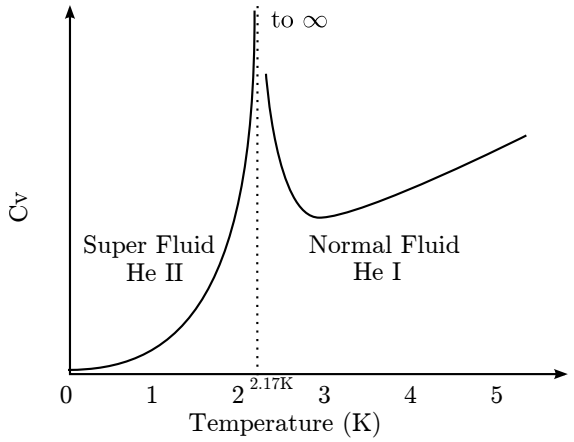

Figure 2.5: C_v - T diagram showing heat capacity peaking over the transition temperature.

With $T_{\text{hot}} \approx 300\text{K}$ and $T_{\text{cold}} \approx 4\text{K}$, the total heat $\dot{Q}$ is still very high for practical purposes, so a intermediary layer of liquid Nitrogen is added so that for the inner dewar only $T_{\text{hot}} \approx 77\text{K}$ (boiling point of Nitrogen)

Baffles or Radiation shields inside the inner dewar reduce radiation down into the liquid. The baffles are cooled by the vapour evaporating off the Helium and so do not just re-emit radiation down.

Another major heat source for the liquid Helium is the support tube, Equation 2.3. So it is constructed out of a thin tube to reduce the cross-sectional area and made from Stainless steel for the low thermal conductivity.

$$\dot{Q}_{\text{conduction}} = \frac{A}{L}\bar{k}\Delta T \tag{2.3}$$

$\bar{k}$ is the average conductivity over the range ΔT.

An example cryostat implementing both a Nitrogen layer and baffles is shown in Figure 2.6.

2.5 Two fluid model

The two fluid model is a phenomenological macroscopic *model* used to explain the characteristics of superfluids, although there is no microscopic theory supporting this.The fluid is treated as two totally inter-penetrating non-interacting fluids. The two distinct fluids are called the components of the fluid. There is no actual physics separation in the normal and super components. The density of the normalfluid and superfluid are related with Equation 2.4

$$\rho = \rho_n + \rho_s \tag{2.4}$$

The subscripts s as the superfluid components and n for the normal component. The superfluid is identified with the ground state energy level Bose-

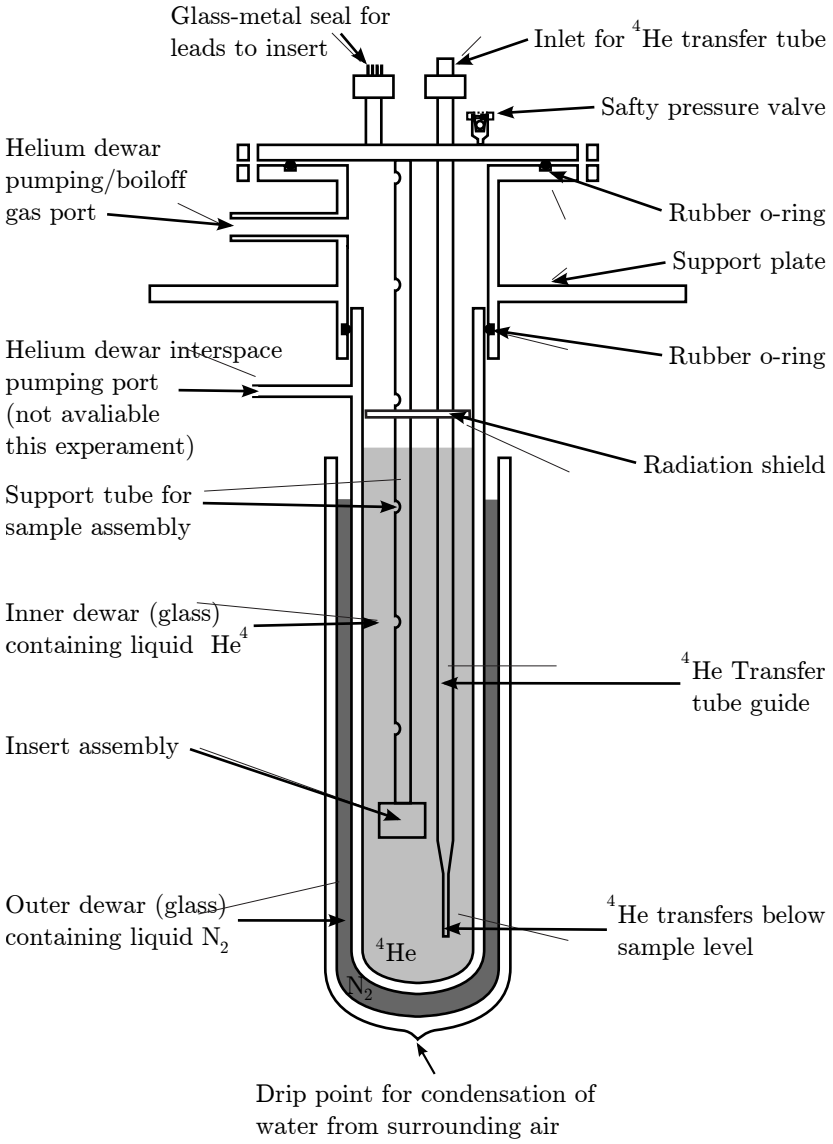

Figure 2.6: Example of dewar used in the lab. Image based on Shaun Fisher's PHYS352 course material [5]. Main alterations are style, formatting, layout, and the addition of the safety valve for the inner dewar.

Einstein condensate and the normal fluid with the excitation above that ground state.

The superfluid component has a velocity $\vec{v}_s$, zero viscosity, zero entropy ($\rightarrow$ zero temperature (third law)), and irrotational flow ($\nabla \times \vec{v}_s$).

While the normal component still behaves classically as a fluid with velocity $\vec{v}_n$ with viscosity and entropy carrying temperature. The proportion of superfluid and normalfluid components change over temperature as more atoms are in the ground state. Figure shows qualitatively the change in proportion of the two components. Above the transition temperature (here T_λ) of superfluidity only the normal component exists so $\rho_n/\rho = 1$. At idealistic $T = 0$, only the superfluid component exists, $\rho_s/\rho = 1$.

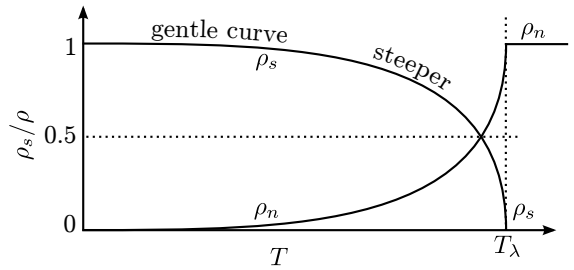

Figure 2.7: Superfluid and normal fluid components changing over temperature.

The ^{4}HeII becomes 'pure at temperatures under about .5k, but the pumping cooling method as a practical limit of about 1K as there are no longer enough atoms evaporating off the gas to reduce the temperature over losses by heat in.

2.6 Counterflow

With a heat source inside a superfluid normalfluid mix, heat converts superfluid to normalfluid, and the normalfluid carries entropy away from the heat source while the rest of the fluid acts as a heatsink. The normalfluid reverts to superfluid at the heatsink. This means that superfluid flows towards the heat source and normalfluid flows away from the heat source. The superfluid is a superconductor of heat and has huge thermal conductivity. There can be no steady state thermal gradients in the superfluid, because of the efficient transition of the heat.

2.7 Thermohydrodynamical Equations

With the hydrodynamical system and the hydrodynamical system that is a superfluid there are 6 Thermohydrodynamical Equations:

- Total fluid density

$$\rho = \rho_n + \rho_s \tag{2.5}$$

- Momentum current density

$$\vec{j} = \rho_n \vec{v}_n + \rho_s \vec{v}_s \tag{2.6}$$

- Entropy conservation

$$\nabla \cdot (\rho S \vec{v}_n) = -\frac{\partial (\rho S)}{\partial t} \tag{2.7}$$

- Acceleration equation

$$\frac{\partial \vec{v}_s}{\partial t} = S\nabla T - \frac{1}{\rho}\nabla P \tag{2.8}$$

- Mass continuity

$$\nabla \cdot \vec{j} = -\frac{\partial \rho}{\partial t} \tag{2.9}$$

- Eulers equation (negating viscosity)

$$\frac{\partial \vec{j}}{\partial t} = -\nabla P \tag{2.10}$$

Hydrodynamical equations for normalfluid have density ρ and pressure P as variables which can be arranged to pressure-density waves. This is just sound, or first sound. But with the thermohydrodynamical equations another pair of variables, entropy S and temperature T can result in a entropy-temperature wave equation, this is the second sound.

$$\frac{\partial^2 S}{\partial t^2} = \underbrace{-\frac{\rho_s}{\rho_n} S^2}_{\text{velocity}} \nabla^2 T \tag{2.11}$$

In this entropy-temperature wave, S and T oscillate in phase.

For second sound waves the velocity squared (c^2) is related to to coefficient in front of the spacial derivative of the variable T, so:

$$c^2 = \frac{\rho_s}{\rho_n} S^2 \left(\frac{\partial T}{\partial S}\right)_p \tag{2.12}$$

as $C_v = T\left(\frac{\partial S}{\partial T}\right)_{\rho,V}$ then

$$c^2 = \frac{\rho_s}{\rho_n} \frac{T S^2}{C_v} \tag{2.13}$$

The second sound wave will have alternating regions of high T to low T while high S to low S and normal component density high ρ_n to low ρ_n then in antiphase low ρ_s to high ρ_s etc. As with the counterflow earlier the $\vec{v}_n$ flows away from T and $\vec{v}_s$ flows towards T. These changes are drawn in Figure 2.8.

In addition to second sound there are third and forth sounds are from applying different boundary conditions the six thermohydrodynamical equations. Third sound is in the thin superfluid films and fourth sound are in superleaks where the normal fluid is clamped because of the viscosity to the porous superleak.

2.8 Second sound

In the propagation of entropy and heat as a wave the temperature is held in the normalfluid component of the superfluid, as $S = 0$ for the superfluid component, see also Figure 2.8. The waves can can be generated by adding cyclic variations of heat, this transmits very well in the normal component and is propagated because of the counterflow and very good thermal conductivity of the superfluid component.

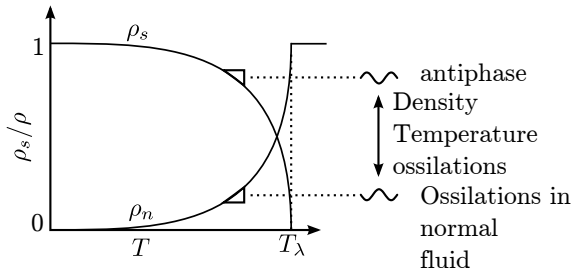

Figure 2.8: Oscillating components of superfluid and normal fluid.

Resonances of second sound will start with high entropy at the heat source and will 'bounce' of the resonance chamber opposite wall at a high region of entropy, unlike compared to first sound in a closed pipe with pressure fixed.

2.9 Cryogenic Fluid Pumping

With nitrogen, the liquid in the transfer dewar is pumped out by opening a heat exchanger valve on the top of the dewar, this boils some of the nitrogen back into the dewar. As the boiled nitrogen is less dense the top space above the liquid is pressurised. The liquid nitrogen is forced out of a transfer tube positioned at the bottom, well below the level of the liquid.

With helium there is no need for a heat exchanger pipe on the transfer dewar as the removable transfer tube is enough to get pressure to pump

helium. Additional complication arise from helium, but these are to conserve wastage.

3 Calibration and Cooling

When cooling the cryogenic environment towards superfluidity by pump cooling, the temperature of the system can be read from values of pressure and looked up in a table. However when heating the system up later the system is not in equilibrium and not strictly on the phase diagram, so only measurements of temperature by resistance in the resonance chamber can be used.

3.1 Experamental Detail

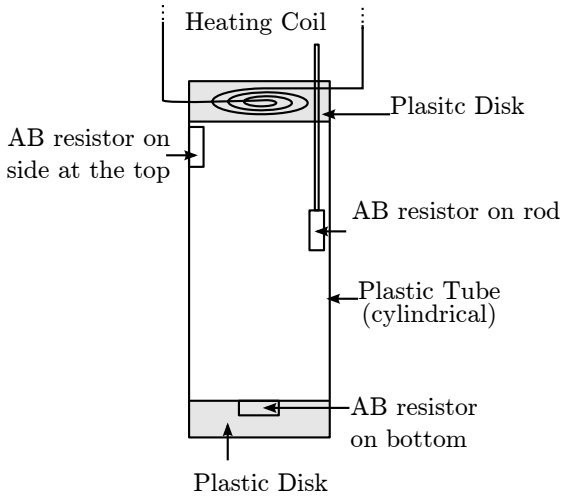

Figure 3.1: Pseudo-physical view of the insert.

Before inserting the insert assembly, Figure 3.1, into the cryostat the length of the resonance chamber is measured using a ruler. The length is used in Section 4.

The insert is inserted into the cryostat. The air is pumped out with an attached portable pump using a valve to the inner dewar. This removes any impurities from the air getting into the ^{4}He dewar, enabling the helium to be recycled afterwards[2]. The air is removed to about 0.8 tor.

The pump is closed off and the vacuum filled with room temperature He from the lab's return line.

From a transfer dewar of liquid nitrogen the outer dewar is filled to very near the top. Using the heat exchange method as described in section 2.9.

The top Allen-Bradley resistor, the one inside the resonance chamber in Figure 3.1, is recorded while the cryostat cools towards $\approx$ 77K. This is a precooling stage. Precooling reduces the latter helium boil off. Sufficient

[2]A cost saving technique, ^{4}He is much more expensive than liquid nitrogen

precooling required about 2 hours of nitrogen. This time is from experience with the lab equipment under guidance from the laboratory demonstrators.

Precooling data is in Table 1 in the appendix.

The operators are already familiar with the operation of the cryostat and the electronics.

Once cool 77K, the Helium is added to the inner dewar using a vacuum insulated transfer U-shaped pipe.

The return line of the inner dewar is open to catch the helium boil off. The helium fills the inner dewar quickly. The pump line is closed, and the pump is turned on. Then the return line is closed as the small valve on the pump line is opened. As the pressure drops the values of the top resistor are recorded for later conversion back to temperature.

During cooling the heating circuit is turned off to aid cooling.

The measurements of resistance are taken with a multimeter, the scale is 1 ohm. The chosen values of pressure to record correspond to approximately evenly distributed values of temperature in Kelvin. The pressure is measured on a modern digital pressure gauge, Figure 3.2, measuring in Tor. The lab book with conversion to temperture are also in Tor, so no pressure conversion is needed.

Figure 3.2: Pressure gauge used in experiment, shown here after pumping on helium.

During further cooling while taking data, the self heating effect of the multimeter measuring the resistance is obvious when changing scales from the 1 ohm setting to the 1k ohm setting. the multimeter is hooked up to an ampmeter to measure the current to measuring the resistor.

The 1 ohm scale uses an 10mA current and the 1k ohm uses a 1μA current. The self heating effect changes the results by a large factor. Data in both the 1 ohm setting and the 1k ohm setting are recorded.

3.2 Results

The data for the full range of measurements from 4.2K down to coldest is graphed in Figure 3.3. For calibration only the region colder than the superfluid boundary temperature is needed, so plot and fitting are done, Figure 3.4.

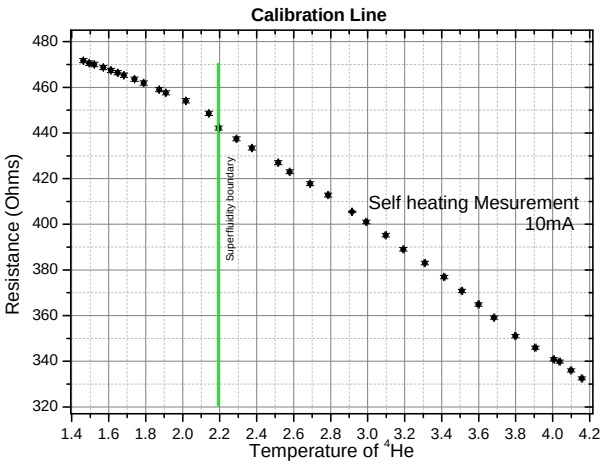

Figure 3.3: Full range of data taken with annotated superfluidity boundary.

For the superfluid the conversion from resistance R in ohms to temperature T in kelvin is

$$\frac{R - (520.89 \pm 1.25)}{(-33.24 \pm 0.72)} = T \tag{3.1}$$

For R in the range $(448 \rightarrow 471)\Omega$. The conversion add an uncertainty of 2.17% but as it is constant conversion formulae over the range $(1.4 \rightarrow 2.3)$K so trends will keep there shape.

A linear relationship for R againt T is not expected although over a short range of ΔT it can be useful.

When the self-heating of the resistor was discovered and the measurement scale changed the additional data collected is plotted with the prior data, Figure . It shows that without the resistor heating itself the resistance is much higher and curved.

However the results are sill useful because the self heating effect is constant. It is quite convenient to use the self-heating calibration because it is liner rather than curved, it is conceptually simpler, meaning conversions are simpler. The non-self heating would yield better detail because of the range of resistances and the better discrimination between measurements.

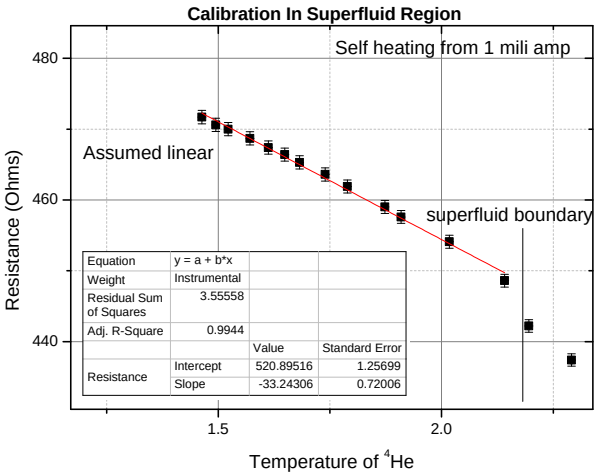

Figure 3.4: Linear plot for calibration of resistance in the superfluid region

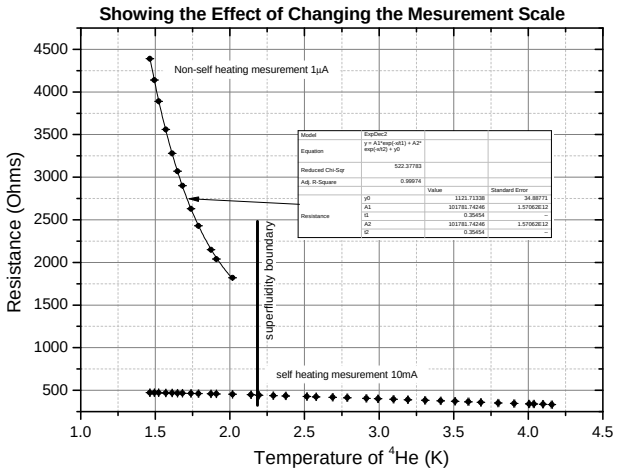

Figure 3.5: Plotting both sets of recoreded resistances showing the dramatic change caused by self heating the resistor.

4 Resonance

Using resonances inside a tube to measure the velocity of second sound. A signal generator heats superfluid in a tube and acts as a reference signal to the phase detector. An Allen-Bradley (AB) resistor measures the fluctuations of temperature of the other side of resonance tube, when the two are in phase, resonance is set up a measurable frequency.

4.1 Theory

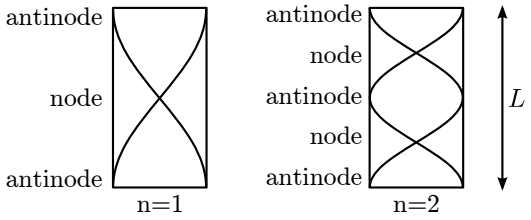

Figure 4.1: Harmonics forming inside the resonance chamber of the cryogenic environment

Inside the resonance tube the second sound resonates down the length L, Figure 4.1. For a wavelength λ, and harmonic n. The fundamental frequency at $n = 1$ is $\lambda/2$. Generalizing for n, Equation 4.1.

$$L = \frac{n\lambda_n}{2} \rightarrow \lambda_n = \frac{2L}{n} \tag{4.1}$$

The velocity from the standard wavelength frequency relation $v = f\lambda$ can be rearranged for λ with $\lambda = \lambda_n$ and $f = f_n$ to get Equation 4.2.

$$v = f_n\lambda_n \rightarrow v = 2f_n\frac{L}{n} \tag{4.2}$$

The heating that adds entropy and temperature for the second sound waves comes for a coil heater connected to a signal generator. The heating requires a bit more theory connecting the power of the coil to the current applied. The heating coil works with ohmic heating, Equations 4.3, 4.4.

$$P = IV \tag{4.3}$$

$$V = IR \tag{4.4}$$

And as 4.4, get to the recognisable result 4.5:

$$P = I^2R \tag{4.5}$$

The current I from the signal generator is varied according to:

$$I = I(t) = I_0\cos(\omega t) \tag{4.6}$$

So from 4.5

$$P = P(t) = I_0^2 \cos^2(\omega t) R \tag{4.7}$$

Using the double angle relation

$$\cos(2\theta) = 2\cos^2(\theta) - 1 \tag{4.8}$$

Re-arranged for $\cos^2(\theta)$:

$$\cos^2(\theta) = \frac{1 + \cos(2\theta)}{2} \tag{4.9}$$

With Equations 4.7 and 4.9 and setting $\theta = \omega t$ then:

$$P = \frac{I_0^2 R^2}{2} \left(1 + \cos(2\omega t)\right) \tag{4.10}$$

By observing the term inside cos() the heating frequency (ω_P power) is twice the drive frequency (ω_I current).

$$\omega_P = 2\omega_I \tag{4.11}$$

This means that:

$$f_n = 2 f_{\text{gennerator}} \tag{4.12}$$

The frequency for the harmonic is twice the frequency used to drive the heating coil, for $f_{\text{gennerator}}$ as the generator frequency. This is heat being produced from the coil for both forwards and backwards current, two peaks of heat for one peak of current, as shown in Figure 4.2.

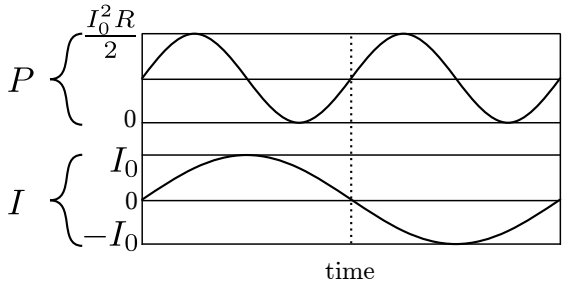

Figure 4.2: The power and current frequencys showing a factor of two gain in frequency.

For v as the propagation velocity from Equation 4.2 above, it means that.

$$v = 2 f_n \frac{L}{n} \tag{4.13}$$

is also

$$v = 4 f_{\text{gen}} \frac{L}{n} \tag{4.14}$$

for $n = 1$

$$v = 4Lf_{\text{gen}} \tag{4.15}$$

For a measurement of different harmonics n and the corresponding frequency f_{gen}, the a linear plot of frequency against harmonic would be the straight line:

$$\underbrace{f_{\text{gen}}}_{\text{y}} = \underbrace{\frac{df_{\text{gen}}}{dn}}_{\text{mx}} n + c \tag{4.16}$$

so

$$v = 4L\frac{df_{\text{gen}}}{dn} \tag{4.17}$$

4.2 Experimental Detail

The insert into the cryostat is built similarly to Figure 3.1 on page 14. Small obstructions in the resonance chamber are the AB resistor on the rod and the AB resistor on the side. The equipment is orientated similarly to Figure 3.1 with the heating coil heating downwards towards the AB resistor for detection.

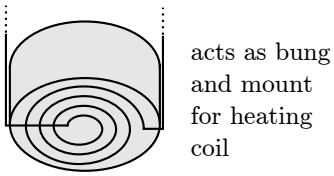

Figure 4.3: Close-up view of the heat bung from Figure 3.1

The heating coil on the top is connected to the circuit and the coil is laid out on the inner surface to maximise a uniform heating surface, Figure 4.3.

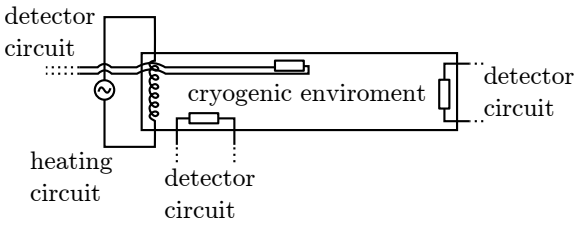

Figure 4.4: Circuit connection available to the cryogenic environment.

The different components are attached to different circuits and are partly swappable, a measurement of resistance can swap between any of the three AB resistors as in Figure 4.4.

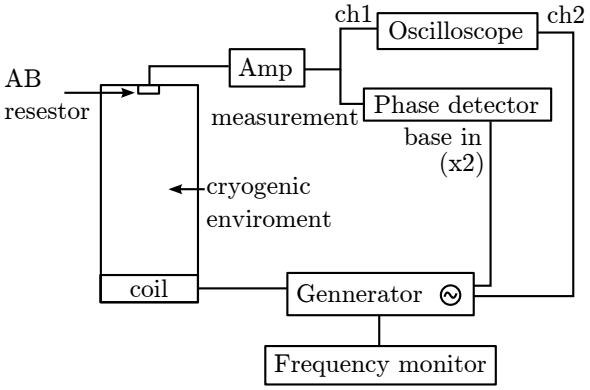

Figure 4.5: Layout of the components connecting apparatus.

For this experiment however the components are connected according to 4.5. The "×2" option is so that the Phase detector uses the effective heating frequency and not just the current frequency as in Equation 4.12.

The experiment is done at the coldest temperature available via pumping, 3.02 Tor.

The frequency generator is connect to the heating circuit. The detector circuit is connected to the lower AB resistor on the opposite face of the resonance chamber. The frequency measurements are taken from a frequency monitor and represent g_{gen}.

A quick search for the first harmonic was conducted by changing the frequency of the generator. From this for scientific precision a range of values around that harmonic and the measurement of the in-phase detection was used to collected data around the peak so that it can be evaluated more precisely.

Using the value for the first harmonic the second harmonic was looked for at twice the fundamental frequency.

$$f_{n=2} = 2f_{n=1} \tag{4.18}$$

More data was taken around the range of the second harmonic in a similar manner to the first.

For the later harmonics, $n = 3, 4, 5 \ldots$, up to $n = 7$, to reduce the time of the experiment, a quicker method in real time conducted by the operator to maximise the detected signal in the phase signal analysis. By looking for the jump of in-phase signal to find the harmonic, then overshooting until a noticeably smaller in-phase signal and moving back until no noticeable difference can be seen. This process is shown in Figure .

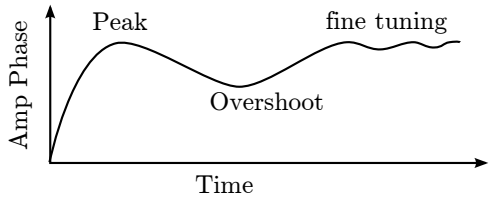

Figure 4.6: Sketch of 'live' method used to find the peaks quickly.

4.3 Results

The length of the tube for resonance is:

$$\boxed{L = (72 \pm 1)\text{mm}} \tag{4.19}$$

The first harmonic was found at around 72 ± 5Hz. The range of measurements around the fundamental yields Figure 4.7. A Beta fitting function was added to find numerically the peak because it fits best with the data.

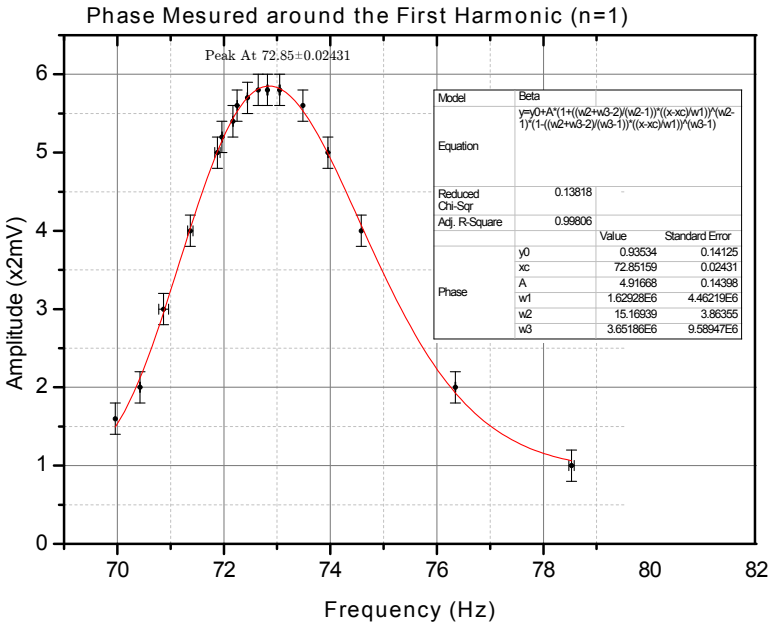

Figure 4.7: Amplitude and frequency around the first harmonic showing a peak at the resonance frequency.

From the graph the first harmonic is:

$$\boxed{F_{n=1} = (72.852 \pm 0.024)\text{Hz}} \tag{4.20}$$

This first peak shows some evidence for second sound in the superfluid.

The second harmonic search began at ≈ 140Hz. Results of taking data yields Figure 4.8. The Lorentz fit works for points near to the peak. However it does not fit all of the data well. The fit is to wide at the sides and to narrow near the peaks centre. But it does have a precise numerical value for the peak.

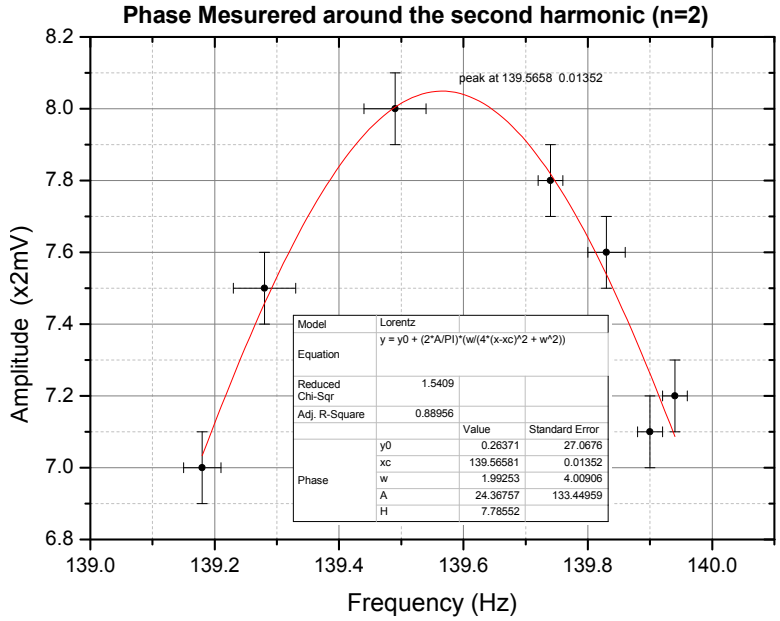

Figure 4.8: Amplitude and frequency around the second harmonic showing a peak at the resonance frequency.

The graph shows that the peak for the second harmonic is:

$$\boxed{f_{n=2} = (139.56 \pm 0.014)\text{Hz}} \tag{4.21}$$

The remaining harmonics are found and recorded. A table of the results up to n=7 is in the appendix in Table 2.

The frequency of the harmonics of the second sound for a straight line when plotted against n. This agrees with Equation 4.17.

A theoretical (0,0) point is added because of the logical extension of Equation 4.17.

The linear fit yields:

$$\boxed{\frac{df_n}{dn} = (68.879 \pm 0.061)\text{Hz}} \tag{4.22}$$

the Intercept of 0 is included in the linear fit because the fitting is better. The high values of $n = 6, 7$ have a slight upwards curl, but the fitting weighting of the errors accounts for this. The fitting still does not have an intercepts

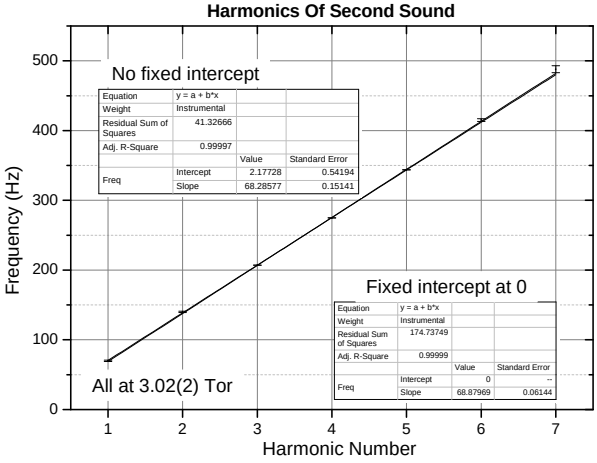

Figure 4.9: The frequency of the generator and the harmonic

that covers 0. This could be from the obstruction in the resonance tube or none-uniform heating across the coil.

Using equation 4.17 with the measured value of $\frac{df_n}{dn}$ from the graph in Figure 4.9 to get:

$$\boxed{v = (19.8372 \pm 0.2761)\text{ms}^{-1}} \tag{4.23}$$

At 3.02 Tor.

An extra graph is produced using Equation 4.14. This uses the individual results (a less accurate method) to calculate the apparent velocity at different harmonics, something that should be constant. However Figure shows that the velocity changes with a 'U' shaped curve with a minimum at $n = 4$. The value for velocity calculated from $\frac{df_n}{dn}$ has uncertainty that cover the range from 19.56 to 20.11, this includes all but the $n = 1$ harmonic. The $n = 1$ harmonic is the most accurate measurement of the graph, so there is another factor that is changing the calculated velocity. It could be the heating from the coil that changes the temperature inside the resonance tube so not all measurements of frequency were at the same temperature, or it could be the wavelength that interferes with the movable resistor at only certain lengths.

4.3.1 Observing Harmonics Shape

As a qualitative exercise, the movable resistor is hooked up to the phase detection circuit. It is lowered starting from the upper position to the middle, then from middle to the lower, Figure 4.11. The signal generator is set for the fundamental frequency.

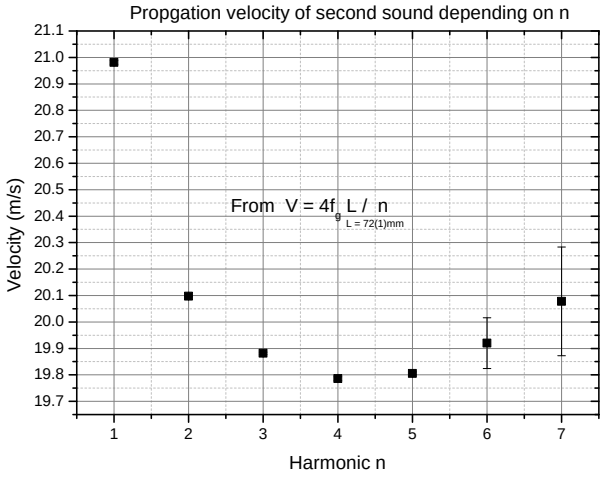

Figure 4.10: The frequency of the generator and the harmonic

It is not possible to get to the very top or very bottom of the resonance tube because of physical limitations.

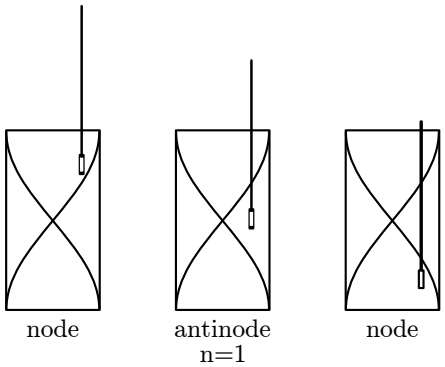

Figure 4.11: The position of the movable resistor changing measuring the

On the oscilloscope it is observed a node is in the middle position and antinodes at the edges.

5 Chasing the Fundamental Harmonic

As a second experiment to measure the change in frequency and so velocity of second sound with changing temperature.

The cryogenic environment is slowly heated up using the already calibrated resistor from section 3 for the temperature measurement.

5.1 Theory

The second sound requires the two fluid model to propagate, but the ratio of superfluid to normal fluid changes over temperature. at $T = T_B$ there is no more superfluid, specifically the velocity depends on the ratio according to:

$$c^2 = \underbrace{\frac{\rho_s}{\rho_n}}_{=0 \text{ at } T>T_B} \cdot \frac{TS^2}{C_v}$$

from Equation 2.13 (page 11).

5.2 Method

The frequency generator is set to the first node. The pipe to the vacuum pump is closed and the pressure from the boiling helium starts to increase.

The liquid helium is not in equilibrium with the vapour and heats up with the net heat flow from the environment. It is not possible to use measurements of pressure to get the temperature, so the Allen Bradley resistor and the calibration is used.

During heating measurements of the resistance and frequency of the first harmonic are taken. The frequency is located using the 'live' method similar to finding the frequency for the $n = \{3, 4, \ldots\}$ harmonics. Excepts at the frequency is constantly dropping the operator predicted the frequency and then without tuning the signal generator a maxima is observed on the phase signal amplifier, this works well when the rate of change of frequency was small, but above ≈ 2.0K the rate of change of frequency was larger and the uncertainty that are approximated the the operator are very large.

The top AB resistor in Figure 3.1 is used for measuring the resistance.

5.3 Results

The Frequency and calculated temperatures are plotted in Figure 5.1. It shows that the velocity depends on the temperature as the frequency of the first harmonic.

At high temperatures, towards T_k, the frequency of the first harmonic drops to 0.

The fitting used is a cubic only because it seems to fit the data well. There is an apparent peak of the frequency at 1.675 ± 0.5, this could be from a beneficial radio of superfluid and normalfluid components.

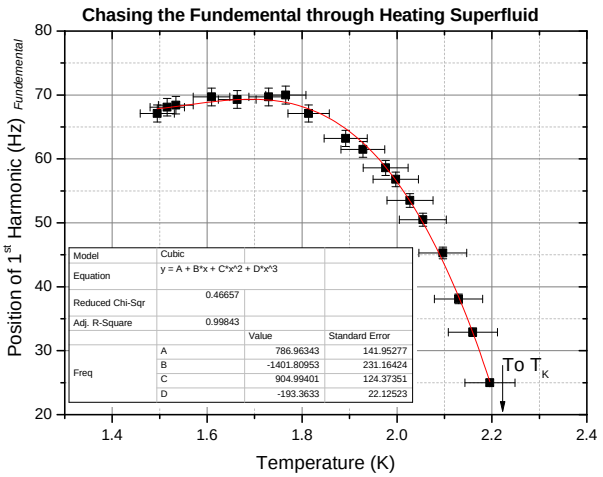

Figure 5.1: Plot of the fundamental frequency against temperature calculated from the resistance of the Allen-Bradley resistor during cooling

6 Conclusion

The presence of second sound was observed on an oscilloscope in liquid superfluid helium (^{4}He-II) at 3.02Tor (1.46K).

The Allen-Bradley resistor used to calibrate the measurement inside the resonance chamber was calibrated at:

$$\frac{R - (520.89 \pm 1.25)}{(-33.24 \pm 0.72)} = T$$

for the range $(448 \to 471)\Omega$, $(1.4 \to 2.3)$K. The conversion add an uncertainty of 2.17%.

The first harmonic at 1.46K in a 72 ± 1mm tube was found at:

$$f_1 = 72.852 \pm 0.024$$

With the additional data of other harmonics, up to the sixth overtone, the velocity of second sound at 1.46K is measured to be:

$$v = (19.8372 \pm 0.2761)\text{ms}^{-1}$$

By following the first harmonic through a temperature change the speed of second sound is observed to drop to zero at the transition temperature to normalfluid from superfluid. This agrees with the theory in Equation 2.13.

6.1 Furtherance

The variable position AB resistor should have had measurements taken over the distance to quantitatively show the node and anitnode layout inside the resonance tube to shows a graph similar to Figure 6.1.

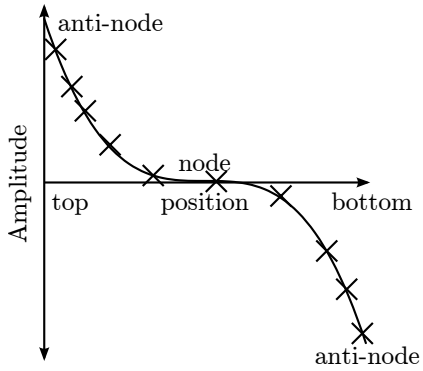

Figure 6.1: Predicted results graph for the measurement of amplitude over position in the resonance chamber for $n = 1$ harmonic.

Uncertainty on the second sound propagation velocity are from the two measured variables, frequency of the n^{th} harmonic, and length.

The major contributor to the uncertainty arises from the length measurement of 72 ± 1mm. A more precise build of the resonance chamber would reduce this 1.38% uncertainty. As the uncertainty in length is from the the in-precise measurement of the ends, a longer resonance tube would reduce the portion $\delta L/L$ used in the uncertainty propagation calcuation for second sound velocity.

The quick method used on the $n > 2$ harmonics could be replaced by the graphing method used for $n = \{1, 2\}$ harmonics for more precise measurement.

The second sound disappears towards T_B, a slower heating method should enable more results to be taken just under T_B to show that the frequency does drop to zero without other dominant factors.

A Background

Studying for a Masters in Physics at Lancaster University, in third year there is a choice to do mini-projects, one of which is about low temperature physics. This report is the result of that series of labs.

A.1 Tools

This document was produced in LaTeX, using Inkscape `http://inkscape.org/` for the diagrams to match the documents style. The scripting language Python `http://python.org/` was used to manipulate data from the origin to convert to LaTeX format.

B Tables

11:30 AM	$67.3 \pm 1\Omega$
11:50 AM	$68.6 \pm 1\Omega$
Cooling continued	lunch break
13:42 AM	$75.8 \pm 1\Omega$

Table 1: Precooling Data

n	Frequency (Hz)
0	0 ± 0
1	72.8515 ± 0.02431
2	139.5658 ± 0.01352
3	207.099 ± 0.05
4	274.8 ± 0.1
5	343.85 ± 0.1
6	415 ± 2
7	488 ± 5

Table 2: Frequencys of the harmonics in second sound.

References

[1] R. J. Donnelly, "The discovery of superfluidity," *Physics Today*.

[2] J. F. Allen and A. D. Misener *Nature*, vol. 141.

[3] Nobelprize.org, "Pyotr kapitsa - biography." Website, 10 Mar 2011. `http://nobelprize.org/nobel_prizes/physics/laureates/1978/kapitsa-bio.html`.

[4] M. Barmatz, "Microgravity scaling theory experiment: Miste science requirements document." BEACON eSpace, 24 Aug 2001. D-17083 `http://hdl.handle.net/2014/13273`.

[5] Shaun Fisher, "Second sound expt fig." Website, 16 Nov 2011. `https://ltg-luvle.lancs.ac.uk/10-11/phys/phys352.nsf`.